Biophysical Journal, Volume *120*

Supplemental information

Unscrambling exit site patterns on the endoplasmic reticulum as a quenched demixing process

Konstantin Speckner, Lorenz Stadler, and Matthias Weiss

Supplementary Figures

Figure S1

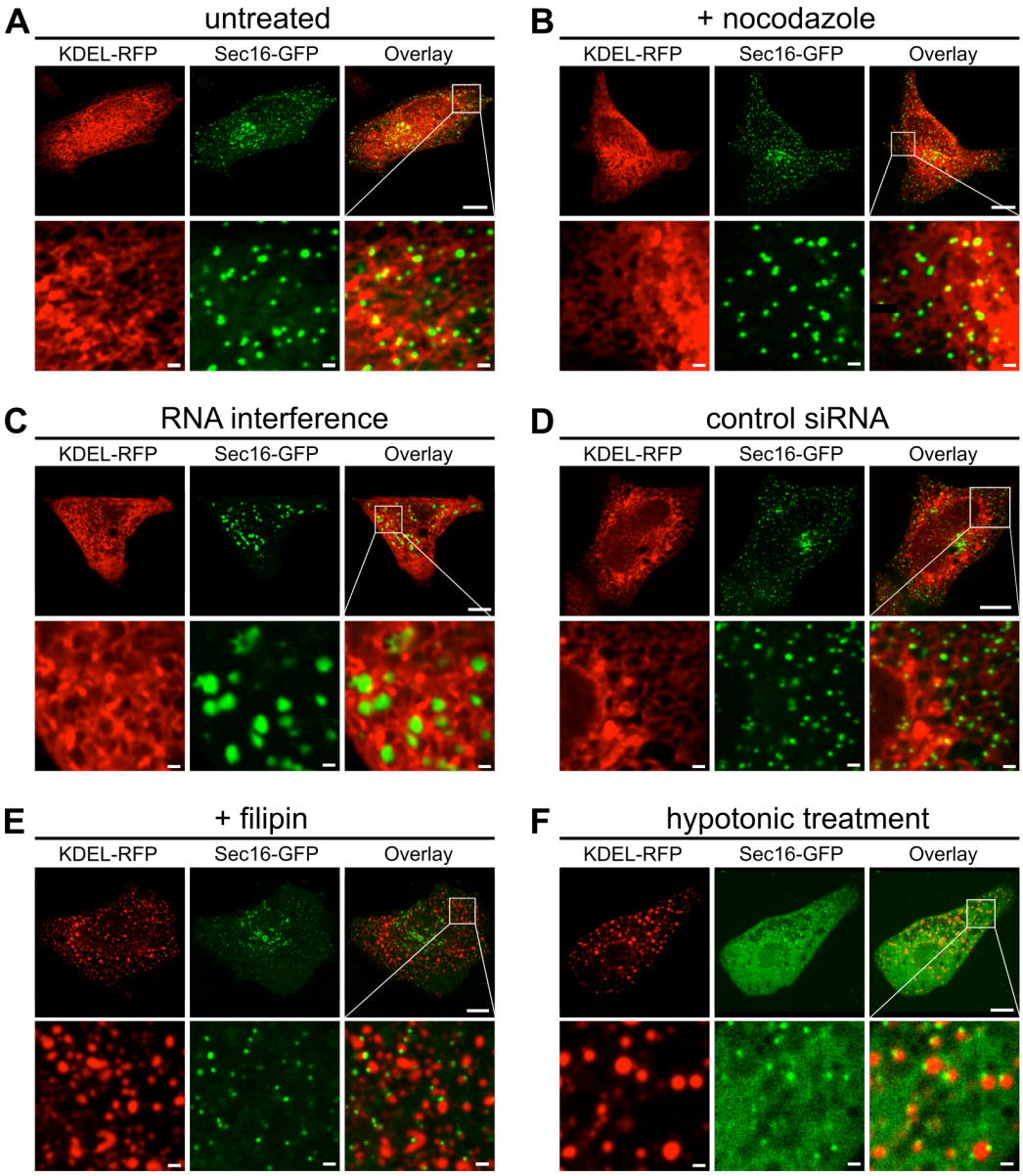

Representative images of the ER (left column, red), the superimposed pattern of ERES (center column, green), and the overlay of both channels (right column) in (A) untreated cells, (B) nocodazole-treated cells, (C) cells in which lunapark proteins have been depleted by RNAi, (D) cells exposed to a negative control siRNA, (E) filipin-treated cells, and (F) cells being immersed to hypotonic medium. Scale bars in all upper panels are 10µm, scale bars in close-ups (lower panels) are 1µm. See Material and Methods for details on each treatment.

Figure S2

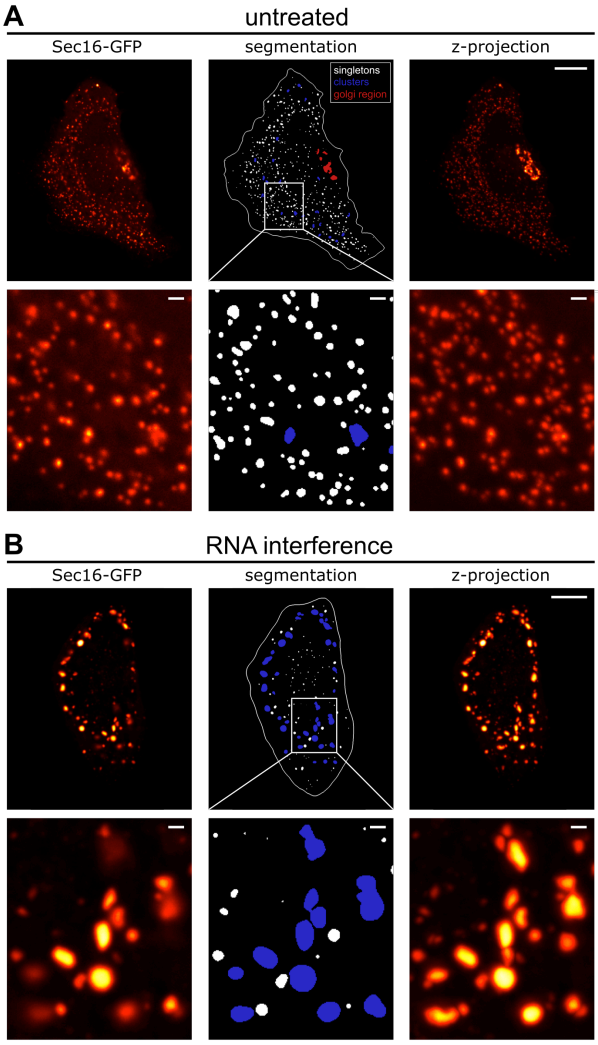

Representative images for the *ilastik*-based segmentation process of (A) untreated cells and (B) after depleting lunapark proteins. The machine learning tool *ilastik* identifies ERES and background from fluorescence images of Sec16-GFP. ERES with less than 150 contributing pixels were classified as singletons (marked in white), larger ones were classified as clusters (marked in blue). Speckled ERES in the putative Golgi region (seen by the maximum z-projection, marked in red) were excluded from further analyses (cf. Materials and Methods). Scale bars in all upper panels are 10µm, scale bars in close-ups (lower panels) are 1µm.

Figure S3

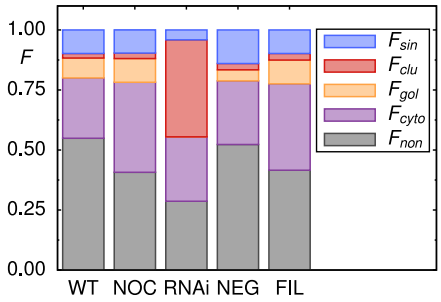

The relative fluorescence share of ERES singletons, F_{sin}, and clusters, F_{clu}, combined with the objects in the putative Golgi region, F_{gol}, is preserved between the different measurement conditions (WT: untreated; NOC: nocodazole; NEG: negative control siRNA; FIL: filipin). Cells in which lunapark proteins have been depleted (RNAi) showed a markedly increased fluorescence with a significantly altered contribution of singletons and clusters. Since Sec16-GFP is also located in the cytosol (F_{cyt}) and on ER membranes outside ERES (F_{non}), major parts of the total fluorescence are not assigned to segmented ERES. See also Materials and Methods for technical details of the analysis.

Figure S4

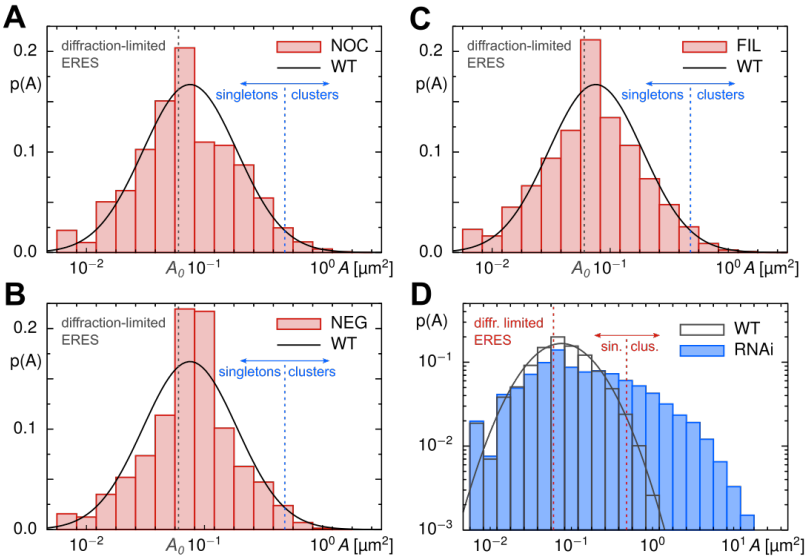

PDF of apparent ERES occupation areas, p(A), obtained for (A) nocodazole-treated cells, (B) cells exposed to a negative control siRNA, and (C) filipin-treated cells show almost the same lognormal shape as for untreated cells (indicated by full black line). Like in Fig. 2 of the main text, dashed vertical lines indicate the diffraction-limited value A_0 (black) and the division line (blue) between singletons and clusters. Clusters were observed in all cases to only make up a fraction of about 2% of all ERES, i.e. singletons contribute the vast majority (cf. Table 1 in the main text). (D) Same data as in Fig. 3B of the main text but in logarithmic plot style to emphasize the changes in p(A) upon RNAi-mediated knockdown of lunapark proteins.

Figure S5

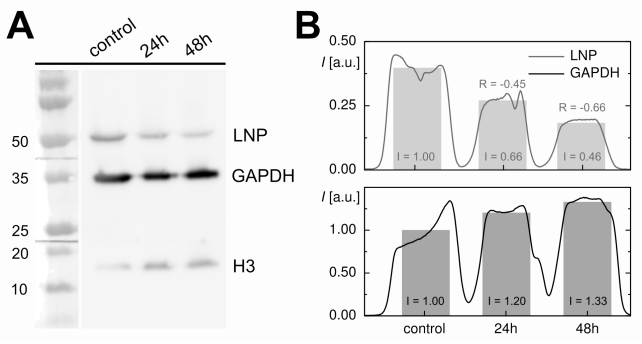

(A) The efficiency of siRNA-induced protein reduction, as evidenced by Western blotting, shows a clear depletion of lunapark proteins (LNP) versus a control band (GAPDH) over a period of 48h. (B) Quantifying the chemiluminescence yielded reductions by 45% after 24h and by 66% after 48h with respect to control cells.

Figure S6

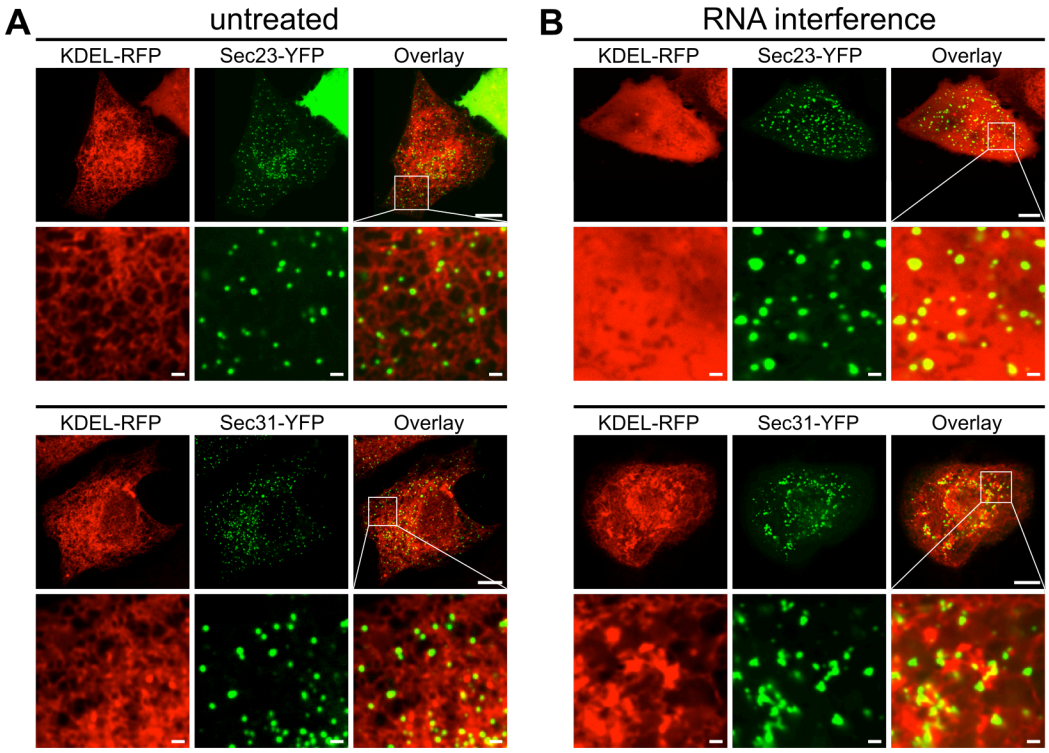

Representative images of the ER (left column, red), the superimposed patterns of ERES (center column, green) and channel overlays (right column) using COPII marker proteins Sec23-YFP or Sec31-YFP for visualizing ERES in (A) untreated cells, (B) cells in which lunapark proteins have been depleted. Untreated cells show dispersed point patters of ERES whereas significantly fewer and larger ERES with a markedly different pattern are observed after lunapark depletion, in agreement with observations on Sec16-GFP (Figs. 1, 3 and S1). Scale bars in all upper panels are 10μm, scale bars in close-ups (lower panels) are 1μm.

Figure S7

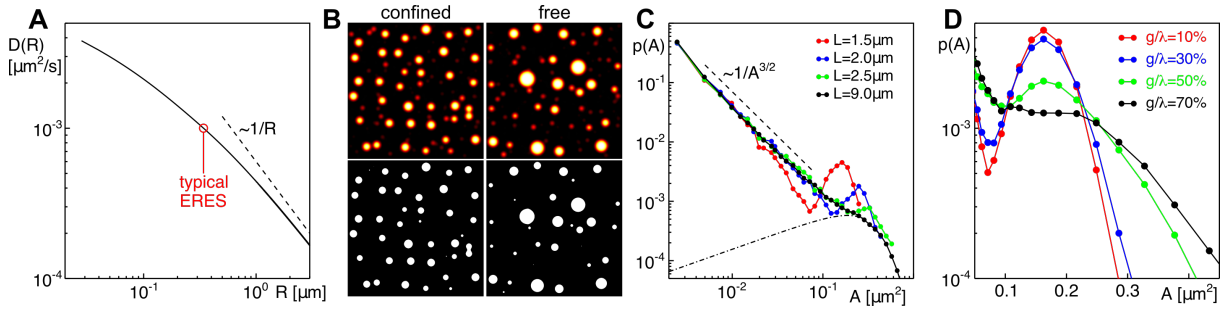

(A) Size-dependent diffusion coefficient, D(R), as used for the simulations (cf. Materials and Methods). The dashed line indicates the asymptotic scaling for very large radii, D~1/R, analogous to the edgewise motion of a thin disk; convergence towards the Saffman-Delbruck limit is observed for small radii. An overall rescaling of D(R) by a constant prefactor was applied to match the experimentally observed mobility of native ERES (indicated by red circle). (B) Representative examples of microscopy-like images (top) obtained by simulations and subsequent blurring, for confined and free diffusion scenarios. Associated binary masks of domains, as obtained by the Matlab routine *bwconncomp*, are shown in the bottom panel. Transfer to microscopy-like images basically masks domains that are significantly smaller than the diffraction limit, highlighting only the larger domains. (C) PDF of domain areas, p(A), as obtained directly from simulations (i.e. without optical blurring) for free diffusion on a square plane at the indicated edge lengths, L. In line with previous predictions, a power-law decay for small domains is observed (dashed line) that becomes entirely masked when transferring the data to microscopy-like images (indicated for L=9μm by the smoothed black dash-dotted line). Reducing the system size, a pronounced peak emerges in p(A) for L=1.5μm. This indicates that virtually all particles on the plane are included in a single domain whose area is determined by the steady-state fraction of membrane-bound particles. The system is well mixed in this limit, i.e. the typical time scale to diffusively explore the plane is smaller than the inverse dissociation rate. (D) PDF of domain areas, p(A), as obtained directly from simulations (i.e. without optical blurring) for confined diffusion on a square plane (L=9μm), dissected into panels with edge length λ=1.5μm. Diffusive exchange of material between neighboring panels was allowed for by a gap of width g in the boundaries, i.e. g<<λ corresponds to the red curve in subfigure C. For growing gap sizes, the pronounced peak due to a single domain per panel subsides and eventually vanishes. The crossover around g~λ/2 matches well to the diameter of domains in the closed panel (400-500nm), i.e. coarse-graining and maturation of the pattern requires that large domains can pass to neighboring panels. Please note the semilogarithmic plot style.